

Influence of Nitrogen Content on Hot Ductility of Nb-and B-added Ultra-low Carbon Steel for Welded Cans[†]

TADA Masaki^{*1} KOJIMA Katsumi^{*2} NAGOSHI Masayasu^{*3}

Abstract:

The influence of nitrogen (N) content on the hot-ductility of combined niobium (Nb) and boron (B) added ultra low-carbon steel was investigated with use of the related commercial steel materials. Nb and B added ultra low-carbon steel in which nitrogen was 0.0048 mass% showed the bottom of ductility around 950°C, which was slightly higher than the Ar₃ transformation temperature. Reducing N content less than 0.0032 mass% improved the hot-ductility around the temperature of 950°C.

Both grain boundary ductile fracture and intragranular brittle fracture were observed in the fractured surface of the tested specimen. MnS, BN and AlN precipitates were observed at the grain boundaries, and the Nb (C, N) precipitates were observed in the ferrite matrix.

These results suggest that the hot-ductility of combined Nb and B added ultra low-carbon steel is deteriorated by both the grain boundary ductile fracture dominated by the MnS, BN, AlN precipitates and the transgranular brittle fracture by the Nb (C, N) precipitates.

1. Introduction

Combined Nb-B added ultra-low carbon steel is used in pail cans and products with similar requirements as this material possesses properties such as minimal change in the circumferential height after expanding, a non-aging property, high weld strength, etc. in addition to the sheet strength necessary in steel

sheets for large-scale welded cans^{1, 2)}.

Among all iron and steel products, these steel sheets for cans are the type of product in which the highest level of surface quality is required. Moreover, with higher requirements placed on materials and study of composition adjustment for manifestation of properties, it is thought that the importance of surface quality will increase in the future.

However, as the hot ductility of these steel decreases remarkably when the nitrogen (N) content increases^{1, 2)}, eliminating cracks during bending-unbending deformation in the slab straightening zone in continuous casting of this steel becomes an issue in the practical manufacturing aspect. In particular, in case the temperature in the straightening zone is around 950°C, which is just slightly higher than the $\gamma \rightarrow \alpha$ transformation temperature, it is thought that the hot ductility change behavior changes greatly depending on the type of precipitates and the precipitation sites.

Since the $\gamma \rightarrow \alpha$ transformation temperature of ultra-low carbon steel is higher than 900°C, the effect of the precipitation behavior of Nb (C, N), BN, etc. on hot ductility is thought to be different from that in low carbon steel.

In this research, the influence of the N content on the hot ductility of combined Nb-B added ultra-low carbon steel was investigated with the aim of stabilizing surface quality, and the controlling mechanism of the hot ductility of this steel was studied. The results are reported in the following.

[†] Originally published in JFE GIHO No. 39 (Feb. 2017), p. 10–14



^{*1} Senior Researcher Manager,
Sheet Products Research Dept.,
Steel Res. Lab.,
JFE Steel



^{*2} General Manager,
Can & Laminated Materials Research Dept.,
Steel Res. Lab.,
JFE Steel



^{*3} Ph. D.,
General Manager,
Nano-Scale Characterization Center,
Functional Materials Solution Div.,
JFE Techno-Research

2. Experimental Procedure

The sample material was a continuous casting material produced by actual production equipment. Its chemical composition is shown in **Table 1**¹⁾. Surface cracks occurred only in the slab of steel No. 1.

A high temperature tensile test was performed to evaluate hot ductility. The test pieces were taken from the 1/4 thickness position from the bottom side to the top side. The direction of tensioning of the test piece was the casting direction (at right angles to the solidification direction). A round-bar test piece with a parallel part diameter of 8 mm and parallel part length of 15 mm was used. The high temperature tensile test was performed in a vacuum, using high frequency induction type thermo-mechanical reproduction test machine (Thermecmaster test machine). The thermal history used in the experiments is shown in **Fig. 1**¹⁾. The tensile test was performed after soaking for at 1420°C for 60 s, followed by rapid cooling to the test temperature and holding at that temperature for 60 s. The strain speed was $2 \times 10^{-3} \text{ s}^{-1}$, which is equivalent to the strain speed in the straightening zone of a continuous casting machine. The reduction in area of the fracture surface after tensile fracture was used in the index for evaluation of hot ductility.

The fracture surface after tensile fracture and precipitates were examined by scanning electron microscope (SEM) observation, transmission electron microscope (TEM) observation, and elemental analysis by energy dispersive X-ray spectrometry (EDX). For the TEM observation, thin film replica were prepared and observation was performed with the specimen supported and fixed with a Cu mesh.

The condition of existence of Nb in the vicinity of the fracture surface was analyzed by X-ray absorption fine structure (XAFS) analysis. Measurement of the

Table 1 Chemical composition of steels used (mass%)

No.	C	Mn	S	sol Al	Nb	B	N
1	0.0016	0.31	0.014	0.047	0.027	0.0012	0.0048
2	0.0022	0.28	0.013	0.048	0.026	0.0011	0.0032
3	0.0010	0.37	0.013	0.044	0.001	0.0013	0.0027

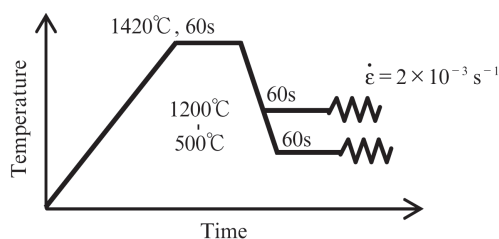


Fig. 1 Schematic diagram of thermo-mechanical testing condition

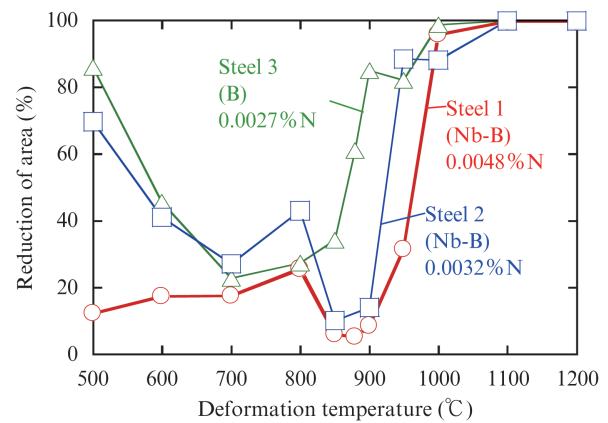


Fig. 2 Effect of nitrogen content on the hot-ductility

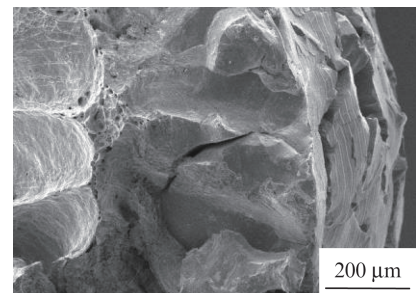


Fig. 3 SEM image of fracture surface of Steel 1 (950°C)

XAFS spectrum was performed by using beamline BL27B, which is installed in the Photon Factory at the High energy accelerator research institute KEK. The XAFS spectrum of the Nb-K absorption edge was measured by the X-ray fluorescence (XRF) yield by using a 7-element semiconductor detector and X-rays monochromatized with a Si (111) two-crystal monochromator. The Nb precipitate percentage in the vicinity of the fracture surface was obtained from an extended X-ray absorption fine structure (EXAFS) analysis^{3, 4)}.

In the analysis of the amounts of precipitated B and Al, the B and Al in the precipitates were evaluated quantitatively by taking samples from the fracture surface of the high temperature tensile test pieces and analyzing the extraction residue after Br methanol extraction.

3. Results of Investigation of Hot Ductility and Precipitates of Combined Nb-B Added Ultra-low Carbon Steel

Figure 2 shows the relationship between the hot working temperature and reduction of area of Steels 1–3¹⁾. In Steel 1, a decrease in hot ductility was observed in the temperature region under 1 000°C. In contrast to Steel 1, the decrease was seen in the temperature region under 950°C with Steel 2, which contained a small

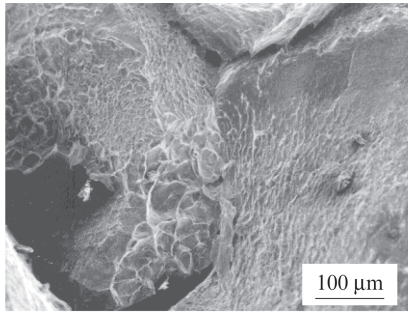


Fig. 4 SEM image of ductile intergranular fracture surface of Steel 1

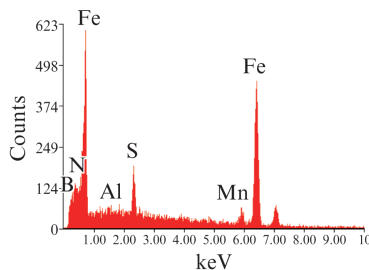
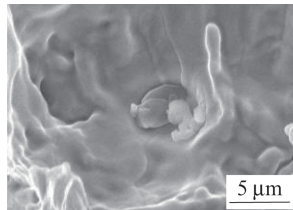


Fig. 5 SEM image and EDX spectrum of precipitates observed in fracture surface of Steel 1 (Deformation temp.: 950°C)

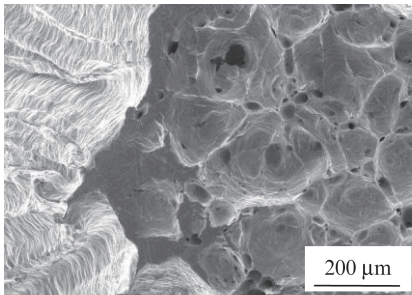


Fig. 6 SEM image of fracture surface of Steel 3 (Deformation temp.: 950°C)

amount of N in comparison with Steel 1, and in the region under 900°C in Steel 3, to which only B was added.

Figure 3¹⁾, **Fig. 4** and **Fig. 5¹⁾** show the result of observation of the fracture surface of Steel 1, which fractured at 950°C, the condition of the precipitates observed in the fracture surface, and the results of EDX analysis of the precipitates, respectively¹⁾. The fracture surface consists of a ductile intergranular fracture surface, which had a dimple morphology, and a brittle fracture surface, and precipitates with a size on the order of 2–5 μm were observed in the ductile inter-

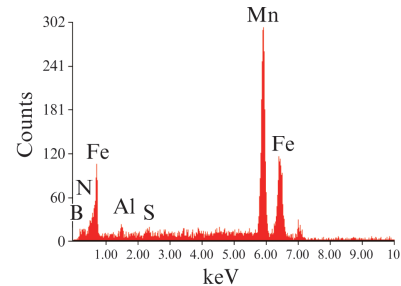
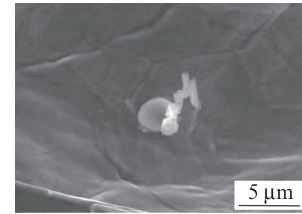


Fig. 7 SEM image and the EDX spectrum of the precipitates observed in fracture surface of Steel 3 (Deformation temp.: 950°C)

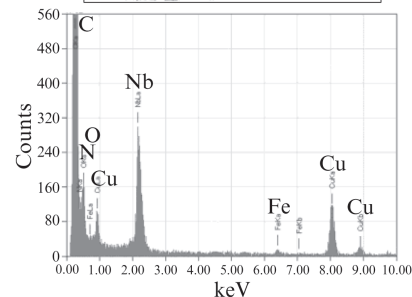
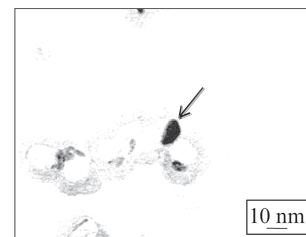


Fig. 8 TEM image and EDX spectrum of precipitates observed by extraction replica in the Steel 1 (Deformation temp.: 950°C)

granular fracture surface. As a result of analysis of the precipitates, Mn, S, B, Al and N were detected.

Figure 6 and **Fig. 7** show the results of observation of the fracture surface of Steel 3, which fractured at 950°C, and the condition of the precipitates observed in this fracture surface and the results of analysis of the precipitates¹⁾. The fracture surface comprises a ductile intergranular fracture surface with a dimple morphology, and precipitates with a size of approximately 5 μm were observed in the fracture surface. As in the case of Steel 1, Mn, S, B, Al and N were detected in the EDX analysis of the precipitates.

To investigate Nb precipitates, TEM observation was performed with thin film replicas. Nb precipitate with a size of approximately 10–20 nm, as shown in **Fig. 8¹⁾**, were observed in crystal grains. The amount

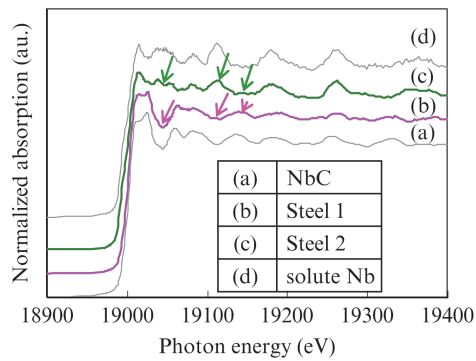


Fig. 9 Normalized Nb-K edge XAFS spectra obtained from (a) NbC reagent, (b) the sample in which 0.012 mass% of 0.027 mass% in Nb content was precipitated as NbC, (c) the sample in which 0.002 mass% of 0.026 mass% in Nb content was precipitated as NbC, and (d) the sample with total Nb in solution

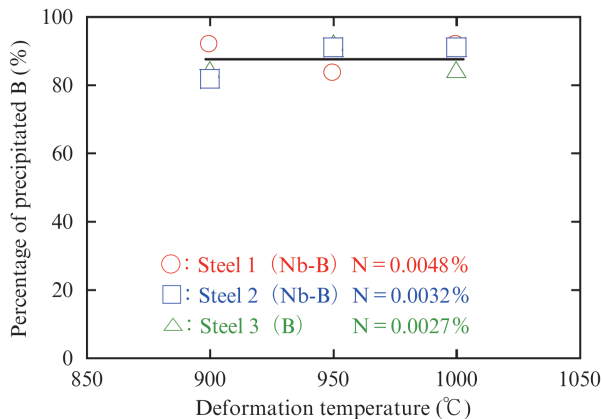


Fig. 10 Effect of the deformation temperature on the fraction of B precipitated as BN in the Steel 1, 2 and 3 determined by chemical analyses

of Nb precipitates was evaluated quantitatively by XAFS, considering the possibility of capture leakage of fine Nb precipitates in the extracted residue method⁵⁾.

Figure 9 shows the XAFS spectra of the Nb-K absorption edge¹⁾. (a) is the reference spectrum of the NbC reagent and (d) is the spectrum of a specimen in which Nb was dissolved in iron. (b) and (c), are the spectrum of a high temperature tensile test piece of Steel 1 with the hot deformation temperature of 900°C, and the spectrum of a high temperature tensile test piece of Steel 2 with the hot deformation temperature of 950°C, respectively.

In spectra (b) and (c) of the high temperature tensile test pieces, the spectral shapes were clearly different; (b) was close to the spectrum (a) of only NbC, while (c) was close to spectrum (d), in which Nb exists in the solid solution state.

Figure 10 shows the relationship between the deformation temperature and the percentage of precipitated B¹⁾. In both the combined Nb-B added steel and the

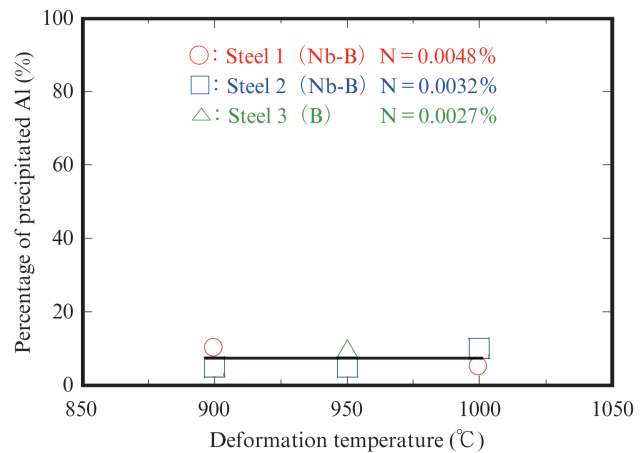


Fig. 11 Effect of the deformation temperature on the fraction of Al on the fraction of Al precipitated as AlN in the Steel 1, 2 and 3 determined by chemical analyses

steel with single addition of B, there was no change in the percentage of precipitated B from 900°C to 1 000°C.

Figure 11 shows the relationship between the deformation temperature and the percentage of precipitated Al¹⁾. In both the combined Nb-B added steel and the steel with single addition of B, precipitation of AlN from 900°C to 1 000°C was small, and was substantially constant at less than 10%.

4. Discussion of Influence of N Addition on Hot Ductility

From Fig. 2, a decrease of ductility is seen at around 950°C, which is slightly above the $\gamma \rightarrow \alpha$ transformation temperature (A_{r3} transformation temperature), when the N content increased from 0.0032 mass% to 0.0048 mass%.

In past research, it has also been reported that a decrease in hot ductility due to the addition of N to low carbon steel occurs due to precipitates^{6, 7)}.

From the results of SEM observation of the fracture surfaces in Fig. 5 and Fig. 7, Mn, S, B, Al and N are detected, and from the results of intragranular TEM observation, Nb, C and N are detected. As precipitates which are observed in combined Nb-B added steel, Nb (C, N), BN, and AlN can be mentioned^{7, 8)}, and it is thought that these have also precipitated in the present experiment. Furthermore, in low carbon steel containing added B and Al, MnS and BN have been observed at grain boundaries⁹⁾. Similarly, it is thought that MnS precipitated as a precipitate in the steel with reduce hot ductility in this experiment.

In order to clarify the influence of precipitates on hot ductility, the changes in the nitrides and carbonitrides of the added elements will be described.

Figure 12 shows the relationship between the reduc-

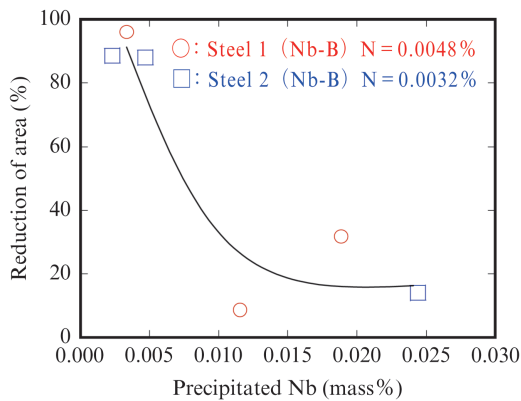


Fig. 12 Effect of Nb content which precipitated as Nb (C, N) on the reduction of area after hot deformation (900~1 000°C)

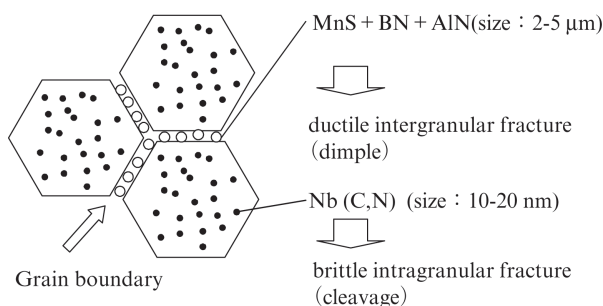


Fig. 13 Schematic diagram showing the mechanism dominating the hot-ductility of Nb and B-added extra low-carbon steel

tion of area and the amount of precipitated Nb¹⁾. The amount of precipitated Nb is calculated by multiplying the Nb concentration of the specimen by the percentage of precipitated Nb. Reduction of area decreased in the specimen with the larger amount of precipitated Nb.

Nb precipitates can be considered to be Nb (C, N), which is observed in Fig. 8. Promotion of fine precipitation of Nb (C, N) in γ grains due to an increase in the N content is considered to be the reason for the increase in precipitated Nb (C, N).

From Fig. 10, the amount of precipitated B does not depend on the N content in either the combined Nb-B added steel or the steel with single addition of B, and from Fig 11, the percentage of precipitated Al also does not depend on the N content. Therefore, it can be thought that an increase in AlN and BN due to an increase in the N content is not the primary cause of the decrease in hot ductility.

From the above, the decrease in hot ductility at around 950°C, which is slightly above the $\gamma \rightarrow \alpha$ transformation temperature (A_{r3} transformation temperature) due to the increase of the N content from 0.0032 mass% to 0.0048 mass% is caused by an increase in the amount of precipitated Nb (C, N).

5. Controlling Mechanism of Hot Ductility of Combined Nb-B Added Ultra-Low Carbon Steel

From the results of SEM observation of the fracture surface and intragranular TEM observation, the precipitates which precipitate at 950°C are considered to be MnS, AlN, BN, Nb (C, N). Furthermore, the cause of the decrease of hot ductility accompanying the increase in the N content is considered to be an increase in the amount of precipitated Nb (C, N). Based on these results, the estimated controlling mechanism of hot ductility in combined Nb-B added ultra-low carbon steel is shown schematically in Fig. 13¹⁾.

The MnS+BN+AlN shown in Fig. 5 precipitates at the grain boundary as the temperature decreases to 950°C.

In this process, in the combined Nb-B added ultra-low carbon steel, hot ductility decreases and grain boundary (intergranular) ductile fracture occurs, with the MnS+BN+AlN that precipitated at the grain boundary as the point of origin.

At the same time, Nb (C, N) is observed by TEM observation in Fig. 8. This Nb (C, N) precipitates inside grains, and transgranular brittle fracture occurs as a result of intragranular hardening¹⁰⁾.

As shown in Fig. 7, MnS+BN+AlN precipitates are observed at the fracture surface in the steel with single addition of B, but a decrease in hot ductility at 950°C is not recognized.

Accordingly, in the combined Nb-B added ultra-low carbon steel, it is thought that hot ductility decreases due to the composite effect of grain boundary (intergranular) ductile fracture due to MnS+BN+AlN precipitation and transgranular brittle fracture accompanying a decrease in the ductility of the ferrite matrix due to intragranular precipitation of Nb (C, N).

6. Conclusion

The new knowledge obtained as a result of this research can be summarized as follows.

- (1) The primary cause of the decrease of hot ductility in combined Nb-B added ultra-low carbon steel in the $\gamma \rightarrow \alpha$ region at above 900°C is considered to be an increase in the amount of precipitated Nb (C, N) due to an increase in the N content.
- (2) With the combined Nb-B added ultra-low carbon steel, MnS+BN+AlN precipitates are observed at the fracture surface and Nb (C, N) is observed in grains after a high temperature tensile test at 950°C. Based on these facts, it is considered that hot ductility decreases in the $\gamma \rightarrow \alpha$ region due to the composite effect of grain boundary ductile

fracture due to MnS+BN+AlN precipitation, and transgranular brittle fracture due to a decrease in the ductility of the ferrite matrix caused by Nb (C, N) precipitated in the grains.

Thus, the phenomenon of slab cracks during continuous casting, which has become a problem with the combined Nb-B added ultra-low carbon steel developed as a steel sheet for cans can be explained by deterioration of hot ductility due to the unique precipitation behavior of precipitates which occurs in this steel, and it is possible to suppress slab cracking by taking countermeasures to control the nitrogen content.

Assurance of the surface quality of steel sheets for cans is extremely important, and it is thought that this knowledge will make a major contribution to stable quality in this field.

The measurements of the XAFS spectra in this research were carried out by joint research with the High energy accelerator research institute KEK. The authors would like to express their appreciation to

KEK and to Professor Emeritus Katsumi Kobayashi and Dr. Noriko Usami for their generous cooperation.

References

- 1) Tada, Masaki; Kojima, Katsumi; Awajiya, Yutaka; Nagoshi, Masayasu; Nakamaru, Hiroki. *Tetsu-to-Hagané*. 2014, vol. 100, p. 1530.
- 2) Tada, Masaki; Kojima, Katsumi; Iwasa, Hiroki; Umemoto, Masashi; Hotta, Eisuke. *Materia Jp*. 2010, vol. 49, p. 81.
- 3) Nagoshi, M.; Kawano, T.; Sato, K.; Funakawa, Y.; Shiozaki, T.; Kobayashi, K. *Physica Scripta*. 2005, T115, p. 480.
- 4) Nagoshi, Masayasu; Aoyama, Tomohiro; Tanaka, Yuji; Ishida, Tomoharu; Kinoshiro, Satoshi; Kobayashi, Katsumi; *ISIJ Int*. 2013, vol. 53, p. 2197.
- 5) Nagoshi, Masayasu; Kawano, Takashi; Sato, Kaoru. *JFE Technical Report*. 2007, no. 9, p. 12.
- 6) Hannerz, N. E. *Trans. Iron Steel Inst. Jpn*. 1985, vol. 25, p. 149.
- 7) Sricharoenchai, Prasonk; Nagasaki, Chihiro; Kihara, Junji. *ISIJ Int*. 1992, vol. 32, p. 1102.
- 8) Cho, Kyung Chul; Mun, Dong Jun; Koo, Yang Mo; Lee, Jae Sang. *Mater. Sci. Eng*. 2011, A528, p. 3556.
- 9) Cho, K. C.; Mun, D. J.; Kang, M. H.; Lee, J. S.; Park, J. K.; Koo, Y. M. *ISIJ Int*. 2010, vol. 50, p. 839.
- 10) Kamada, Yoshihiko; Ohtani, Hiroo. *Tetsu-to-Hagané*. 1990, vol. 76, p. 104.